JMEPEG (2012) 21:500–507
DOI: 10.1007/s11665-011-9939-7

1059-9495/$19.00

The Effects of Square and Circular Die-Orifices on the Performance of Combined Extrusion-Forging Process

S. Sezek, C. Misirli, B. Aksakal, and Y. Can

(Submitted April 21, 2010; in revised form January 25, 2011)

The upper bound (UBM) and finite element methods (FEM) both coupled with experiments have been conducted to analyze forming performance, load prediction, and pressure analyses in a combined extrusion-forging process using square and circular die orifices. The forming load was predicted by the UBM and the pressure distribution was analyzed by FEM and the performance of both the methods was compared to each other. The required extrusion forging force for square die orifice was found to be higher than in the circular die orifice. The highest pressures occurred on the edges of the square and circular orifices and the pressures increased with increasing friction and deformation. Although extrusion force predictions were found to be slightly higher in UBM than FEM, they were in good agreement with experimental results. The present analyses showed that UBM can be used in rapid prediction of required extrusion-forging loads and material flow, and FEM is more suitable to use in pressure distribution analysis for production of square and cylindrical parts.

Keywords extrusion, FEM, forging, forming loads, upper bound

1. Introduction

Nowadays, many engineering parts, especially those used in the automotive, aviation, and space industries, are manufactured by extrusion or forging processes. The forging-extrusion is a combined process as its name implies and mostly used in metal forming processes for pre-forming or near net shaping of many industrial parts used especially in automotive and aerospace industries. In the simplest type of forging-extrusion process, a cylindrical billet is compressed between two parallel overhanging dies and material flows axisymmetrically.

Because of their industrial importance, the combined extrusion and forging processes were investigated by many researchers. The first study in the literature goes back to the 1960s (Ref 1, 2). Both open and closed-die complex flow in extrusion-forging was introduced (Ref 3). An analytical expression to predict the deformation mode during the formation of a flange with an extruded central burst was developed (Ref 4) and a numerical study at the early stage of forging-extrusion using elastoplastic finite element analysis to show the influence of die hole diameter on forming load (Ref 5) opened up further studies in metalworking arena. The influence of orifice diameter on forging pressure was also evaluated using the upper bound method, UBM (Ref 6). The results revealed that increasing orifice diameter caused an early transition from the first to the last stage of deformation. Effect of orifice angle and fillet radius of upper die on deforming body was shown that the fillet radius has no influence on the compression forces, but the friction had a significant effect as high as 15-20% on extrusion forces (Ref 7). The formability, influence of die geometry, and friction conditions in extrusion forging have been evaluated in similar manner (Ref 8). The influence of die parameters, e.g., different draft angles and die radii, on the deformation of extrusion-forging was analyzed and the results also indicated that the draft angle and the billet radius had great influence on extrusion load, the boss height, the flange width and the strain distribution at different deformation levels (Ref 9).

Metal flow behavior in forging-extrusion of rectangular billets for the grooved dies using FEM was investigated (Ref 10) and polygonal blocks were deformed by open die forging using another powerful tool of UBM (Ref 11). As a continuation of that process an experimental and theoretical work was also introduced to analyze cold and hot plate rolling using dual stream functions, DSF (Ref 12). Forward extrusion of clover sections from lead billet has been investigated and good agreement was found between the measured and the predicted loads (Ref 13). The flow pattern of a billet at each punch stroke was analyzed and, square grids are inscribed on the surface formed by cutting the billet longitudinally via UBM. The influence of friction on various metal-forming processes was reported (Ref 14). A combined upper bound and slab method was proposed for estimating the deformation load in cold rod extrusion of aluminum and lead using an optimum curved die profile (Ref 15). An experimental characterization of the volume defects in extrusion has been estimated and it appeared to be very sensitive to flow conditions (Ref 16). In another work, 3D FEM analysis predicting the stress concentration in the contact area between the dies and the ring

S. Sezek, Vocational School of Askale, Ataturk University, Erzurum, Turkey; **C. Misirli** and **Y. Can**, Engineering Faculty, Mechanical Engineering, Trakya University, Edirne, Turkey; and **B. Aksakal**, Department of Metallurgy and Materials Engineering, Firat University, Technology Faculty, Elazig, Turkey. Contact e-mail: b.aksakal@firat.edu.tr.

workpiece was evaluated at any time of the process while the non-contact area having relatively smaller pressures (Ref 17, 18).

Although several studies have been performed on extrusion-forging process, none has dealt with deformation behavior fully by comparing the alternative theoretical solutions and predictions using the FEM and UBM together with experiments. In this study, to improve design aspects for the production of cylindrical and square cross sections, using a combined forging-extrusion process, the deformation behavior and the influence of orifice geometry on metal flow and load requirements were analyzed theoretically and experimentally, and the results were in good agreement.

2. Description of the Process

In the simplest type of forging-extrusion process, a cylindrical billet is compressed between two parallel overhanging dies. The process is basically classified as open die forging-extrusion as illustrated in Fig. 1(a), (b). The friction between the tool and the material interface is assumed to be low and the complete deformation is considered in zones I and II (Fig. 1a). In Zone I, material flows radially and extrusion through the orifice does not occur, thus the total height of workpiece decreases with a reduction in flange. The Zone II begins to move when energy is required to overcome the frictional resistance at the tool-workpiece interface. In Zone II, the increasing size of surface area also causes an increase in frictional resistance and the workpiece is then extruded.

3. Theoretical Solutions

In many metal-forming processes, such as forging and extrusion, the metal flow changes according to the die geometry and the type of material. Complex shapes and consequential flow mechanisms make the analysis even harder when calculating the required forming forces and stresses (Ref 6). During the flow of workpiece throughout the orifice due to excessive plastic deformation and inhomogeneous deformation, the cracks and fracture of the grains may well take place. In order to avoid such problems, the metal flow and stress analysis ought to be carried out to determine the optimum process parameters before the production routes. UBM is a minimum energy method in which kinematically admissible velocity fields are built to describe the metal flow and is very useful for rapid forming load predictions in many metal-forming applications (Ref 11, 12), as FEM are used widely for stress analysis in metalworking processes.

A numerical approach to such a combined forging-extrusion process is applied using FEM on the base of the axis as illustrated in Fig. 1. In addition, the energy requirements are calculated using UBM. For this, the solution is derived to explain the energy required to overcome friction and to deform the workpiece plastically. Thus, the total power is calculated and the minimum energy requirement is found by minimizing the total energy as the detailed narration of the method is described elsewhere (Ref 6, 11, 12). The previous works, in general, dealt with metal flow predictions by UBM or either stress analysis by FEM individually. However in this study, both the methods were used and compared to each other in predicting the forming energy requirement, extrusion load and stress analysis, respectively.

3.1 Modelling of Extrusion-Forging Process

In such extrusion-forging process, a cylindrical workpiece was located in between a pair of plain and hollowed cylindrical lower dies and upper dies with a square orifice. They are moved downward with a velocity of V_0 to squeeze the workpiece (Fig. 1a). The Cartesian coordinate system was used, and it was assumed that the central upper surface of the workpiece and the center of hollowed upper dies coincided. At bottom center of the workpiece, the vertical axis, z, and the axis of hollow also is coincided. The initial and final dimensions of the workpiece are illustrated in Fig. 1(b).

3.2 The Material Flow

During the extrusion-forging process, as the upper die moves vertically downward with a velocity of $V_0 = -1$, the workpiece in Zone II moves upwards at a unit velocity of $V_D = 1$. The material flow in three dimensions is expressed by the velocity fields. The radial velocity components as illustrated in Fig. 2 are determined using the volume constancy. The other known equations of upper bound method such as internal energy dissipation, shear, total energy equations are given elsewhere (Ref 6, 11, 13) for various forming operations. Using

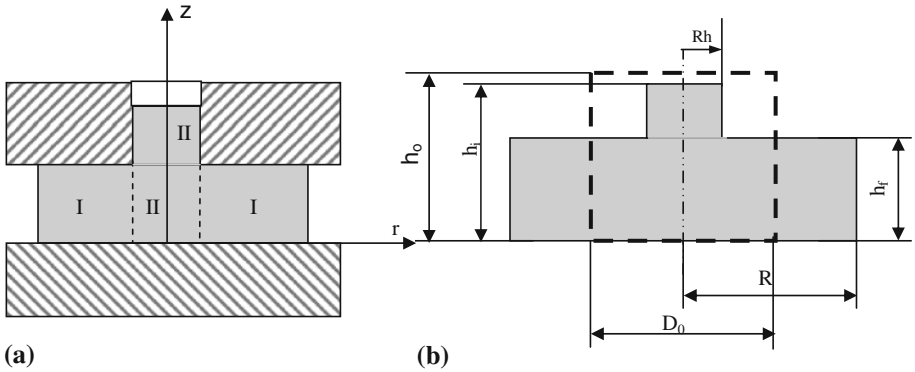

Fig. 1 (a) Deformation zones in extrusion-forging process, (b) undeformed (bold dashed) and deformed (filled) geometries

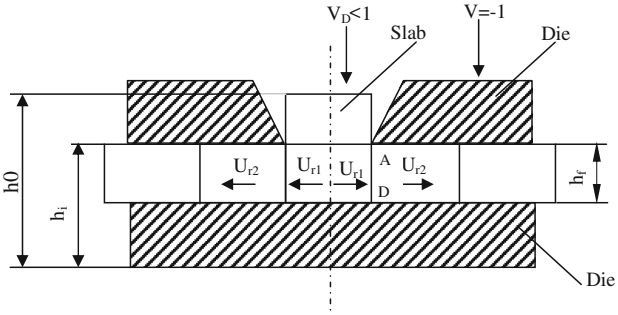

Fig. 2 The velocity discontinuities

such equations in forging-extrusion process for the current boundary conditions, in the center, $0 \le r \le R_h$, the radial, axial, and circumferential velocities (U_r, V_θ, and W_z, respectively) are derived for Zone II and given below:

$$U_{r1} = \frac{V_D \cdot r}{2h} \quad W_{Z1} = -\frac{V_D \cdot z}{h} \quad V_{\theta 1} = 0 \qquad \text{(Eq 1)}$$

The velocities for Zone I, $R_h \le r \le R$, are then determined as:

$$U_{r2} = \frac{r}{2h}\left[1 - \left(\frac{R_h}{r}\right)^2 (1 - V_D)\right]$$
$$W_{r2} = -\frac{V_D}{h} \cdot z \qquad \text{(Eq 2)}$$
$$V_{\theta 2} = 0$$

Using these velocity components, the strain rates in cylindrical coordinates are determined and given in Eq 3.

$$\dot{\varepsilon}_{rr} = \frac{dU_r}{dr} = \frac{1}{2h}\left[1 + \left(\frac{R_h}{r}\right)^2 (1 - V_D)\right]$$
$$\dot{\varepsilon}_{vv} = \frac{U_r}{r} = \frac{1}{2h}\left[1 - \left(\frac{R_h}{r}\right)^2 (1 - V_D)\right] \qquad \text{(Eq 3)}$$
$$\dot{\varepsilon}_{zz} = \frac{dW}{dz} = -\frac{1}{h}$$

3.3 Internal Energy Requirement

By substituting the derivative products of Eq 2 and 3 into the following Eq 4,

$$W_D = \frac{2\sigma}{\sqrt{3}} \int_V \sqrt{\frac{1}{2}\left(\dot{\varepsilon}_{rr}^2 + \dot{\varepsilon}_{\theta\theta}^2 + \dot{\varepsilon}_{zz}^2\right) + \dot{\varepsilon}_{rz}^2 + \dot{\varepsilon}_{r\theta}^2 + \dot{\varepsilon}_{z\theta}^2}\, dV \qquad \text{(Eq 4)}$$

The ideal deformation energy for the first zone, Zone I, is then computed. In flange, the ideal deformation energy for Zone I, and the ideal deformation energy for Zone II, and finally the total ideal deformation energy is computed using the following Eq 5,

$$W_D = W_{D1} + W_{D2} \qquad \text{(Eq 5)}$$

where W_{D1} and W_{D2} are;

$$W_{D1} = \frac{2\sigma}{\sqrt{3}} \int \sqrt{\frac{1}{2}\left(\frac{V_D^2}{4h^2} + \frac{V_D^2}{4h^2} + \frac{V_D^2}{h^2}\right)}\, r dr d\theta dz \qquad \text{(Eq 6)}$$

$$W_{D2} = \frac{2\sigma}{\sqrt{3}} \int \sqrt{\frac{1}{2}\left[\left(\frac{1}{2h}\left(1 + \frac{R_A^2}{R^2}\right)\right)^2 + \left(\frac{1}{2h}\left(1 - \frac{R_A^2}{R^2}\right)\right)^2 + \frac{1}{h^2}\right]} \times r dr d\theta dz \qquad \text{(Eq 7)}$$

Here, $R_A = R_h\sqrt{1 - V_D}$.

3.4 Energy Required to Overcome Friction

Due to the friction on the upper and lower contact surfaces of deforming body, the energy distribution is then given as:

$$\dot{E}_F = \int_0^{R_h} \tau |\Delta V|\, dS \qquad \text{(Eq 8)}$$

where E_F is the energy dissipated due to friction, m is the friction factor, and τ is shear strength. By substituting ($m \cdot \sigma/\sqrt{3}$) into shear stress and boundary conditions (from 0 to R_h) into Eq 8, the velocity discontinuity in the first region becomes:

$$W_{F1} = \frac{2\pi m\sigma}{h\sqrt{3}}\left[\frac{V_D R_h^3}{6}\right] \qquad \text{(Eq 9)}$$

The relative velocity on the contact surface:

$$W_{F2} = m\frac{\sigma}{\sqrt{3}} \int_{R_h}^{R} |\Delta V| R\, dR\, d\theta \qquad \text{(Eq 10)}$$

If Eq 9 and 10 are substituted into Eq 11 and is integrated along the boundaries of upper and lower contact surfaces, finally the total energy consumption for the friction is found as follows:

$$W_F = W_{F1} + W_{F2} \qquad \text{(Eq 11)}$$

3.5 The Energy Along Velocity Discontinuities

As seen in Fig. 2, along the line AD, where it is divided vertically by Zones I and II (Fig. 1a), the velocity, ΔV, determined from the relative velocity and the energy requirement along the velocity discontinuities is obtained as follows:

$$W_S = \int_S \tau |\Delta V|\, dS \qquad \text{(Eq 12)}$$

The total required energy is determined by summing the Eq 11 and 12;

$$W_{T1} = W_D + W_F + W_S \qquad \text{(Eq 13)}$$

The flow stress of the deforming body was determined and by dividing the contact surface area ($A = \pi\,(R^2 - R_h^2)$) by the

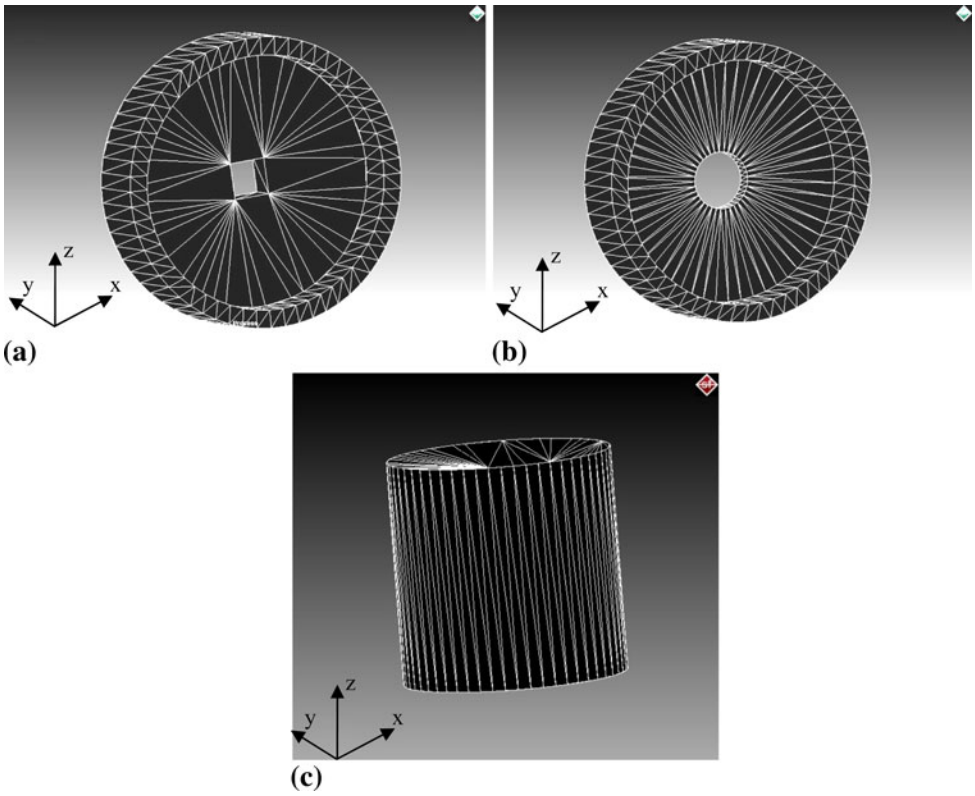

Fig. 3 FEM meshing for (a) square die-orifice, (b) circular die-orifice, and (c) workpiece

Table 1 Material properties of workpiece and die used in the analysis

Properties	FEM	Meshing elements	Increment frequency	Strain change	Elasticity modulus, GPa	Poisson's rate	Density, kg/m^3	Thermal expansion, 1/K	Yield stress ($\sigma_{0,2}$), MPa
Workpiece	3D	6000	5	0.4	14	0.3	1136	2.93e−005	45
Dies	3D	8420	5	0.4	293	0.3	9459	1.15e−005	56.54

unit velocity, then finally the relative pressure ratio of the deforming material becomes as follows:

$$\frac{P}{\sigma} = \frac{1}{R^2 - R_h^2}\left\{\frac{R_A^2}{\sqrt{3}}\left(\sqrt{3\left(\frac{R}{R_A}\right)^4+1} - \sqrt{3\left(\frac{R_h}{R_A}\right)^4+1} - \mathrm{Ln}\left[\left(\frac{R_h}{R_A}\right)^2\left\{\frac{\sqrt{3\left(\frac{R}{R_A}\right)^4+1}+1}{\sqrt{3\left(\frac{R_h}{R_A}\right)^4+1}+1}\right\}\right]\right) + V_D \cdot R_h^2 + \frac{V_D R_h^3}{3h\sqrt{3}} + \frac{R_h h}{\sqrt{3}}(1 - V_D) + \frac{2m}{\sqrt{3}}\left[\frac{R^3 - R_h^3}{3} + R_A^2(R - R_h) + \frac{V_D R_h^3}{6}\right]\right\} \quad \text{(Eq 14)}$$

where V_D is the vertical velocity of the extruded material in the center, $V_D = \frac{H_i - H_o}{H_i - h}$ H_i is the original workpiece height, H_0, before the deformation, and h is the total flange height. The total computing time for a single deformation step took only 15 s on a 2.6 MHz core duo PC. The required extrusion loads can be found by minimizing Eq 14 with respect to V_D.

3.6 Modeling of the Extrusion-Forging by FEM

The extrusion-forging process was modelled using FEM for cylindrical and square orifices as related meshing is illustrated in Fig. 3(a) to (c). The program was run with both load and displacement by applying as high as 50% deformation. The ram speed was kept constant at 5 mm/s and modelled in "forward extrusion" using the MSC-Super-Forge. The total computing time to calculate the stress distribution for a single deformation step took 5 min on a 2.6 MHz Core Duo PC. The varieties in flow cause some difficulties in calculating the complex flow mechanisms, especially forming load and stress distributions. As the simulation parameters are given in Table 1, the commercial lead having the dimensions 25 mm in diameter and 25 mm in height was used for the analysis. The MSC Femutech library of 3D model consists of 6000 quadratic AFQ (Advancing Front Quad) elements and 25000 nodes with increment frequency of 5 and 0.4. The process was first run in elastic zone, then in plastic zone, and the mesh discontinuity was organized by considering the orifice shapes. Distortions occurred particularly during workpiece metal flow at near the edges of the orifice where high friction is present and therefore the number of elements was increased. This is the reason for using re-meshing of quadratic elements at the edges to

prevent such discontinuity. The remeshing sensitivity was 9×10^{-4} m and the number of elements was increased as high as 600 after remeshing. A contact element is defined by considering friction and the exact friction is also defined between the material and dies. The plastic shear factor was taken as the interface friction factor in the analysis.

4. Experiments

Cylindrical lead billets and dies were machined with high accuracy using CNC tools and machines. The workpieces were compressed between two parallel flat dies with the upper die containing circular and square orifices having the same cross-sectional area. The workpiece was extruded through the circular and square dies by the use of a 150 kN hydraulic press. In such extrusion-forging process, as the thickness of the workpiece decreases the lower diameter, $2R$, increases perpendicularly to the force direction while the material moves upwards and fills the upper die orifice.

Cylindrical lead workpieces having the dimensions 25 mm in diameter and 25 mm in height, machined from the extruded lead bars. Two different dies, at circular and square geometries, were machined and manufactured from DIN 1.2344 steel (0.4%C, 0.4Mn, 5.25%Cr, 1.35%Mo, 1.0%V, 1.1%Si, $<$0.03%P and S). As shown in Fig. 4, the circular orifices, which has 10 mm of diameter, and the square orifice has the same cross-sectional areas of 78.5 mm^2, and hardness of 48 HRC and flow stress of 45 MPa. After centrally positioning of the billet on the lower die, the upper die was compressed downwards with 5 mm/s ram speed. The height reduction (%) was calculated when the upper platen has contacted the upper surface of the workpiece. The extrusion-forging forces were recorded automatically by a data acquisition system (Trapezium). Figure 5 shows the produced experimental workpieces as received (a), forged (b), and extruded by the circular (c) and square (d) orifice dies at the same reduction ratios.

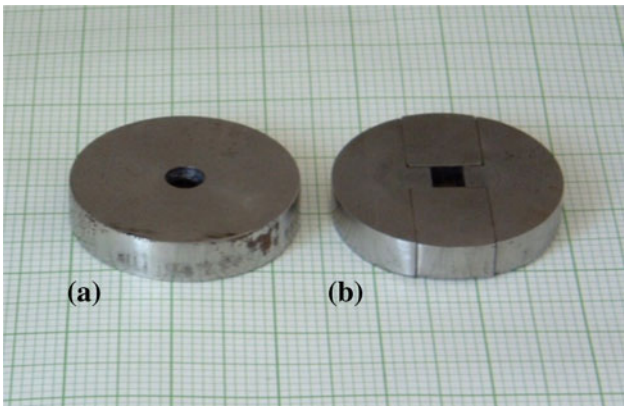

Fig. 4 Die orifices used in experiments

5. Results and Discussion

The upper bound and finite element methods were used for a combined process of extrusion-forging process for producing the square and circular cross sections. These tools have been used for the load prediction, numerical modelling, and stress analyses, respectively. Although the current phenomenon is similar with the earlier studies (Ref 4, 6, 7) here, two different orifices and two different methods were used and compared to each other. The upper bound statement is established to predict the forming energy and thus the forming loads required to overcome internal deformation and friction occur between the extruded material and the dies. The total power is calculated via the UBM and the minimum energy requirement is calculated by minimizing the total energy. Then the pressure analyses were carried out and the calculated load requirements are compared with both solutions of UBM and FEM. Die shape, rapid prediction of loads, and stresses are very important in such forming operations; therefore, two different die shapes, having circular and cylindrical orifices, with various friction factors have been analyzed theoretically and compared to experiments.

5.1 Square Die Orifice

Figure 6(a-c) shows the pressure distributions obtained by FEM analysis for 10, 30, and 50%, respectively, deformations during extrusion-forging process using the square die orifice. As seen from the figure, the maximum pressure is 3,235 N/mm^2 for 10% deformation in square orifice and it increased with increasing deformation, e.g., increased up to 3,723 N/mm^2 for 50% deformation (Fig. 6c) along the edges of square orifice due to the shear stress concentrations. This can be referred to as the forming energy exerted on the upper die due to friction and the external energy applied by the punch to the upper die.

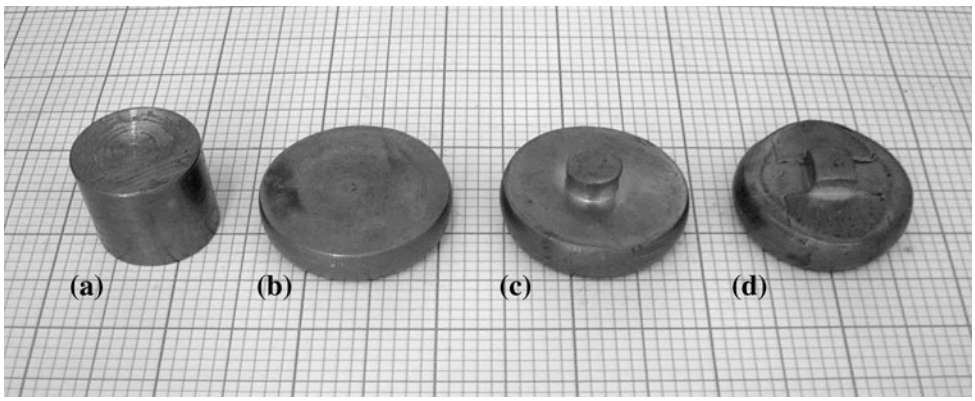

Fig. 5 Experimentally forged-extruded samples; (a) undeformed, b) open-die, (c) by circular orifice, (d) by square orifice

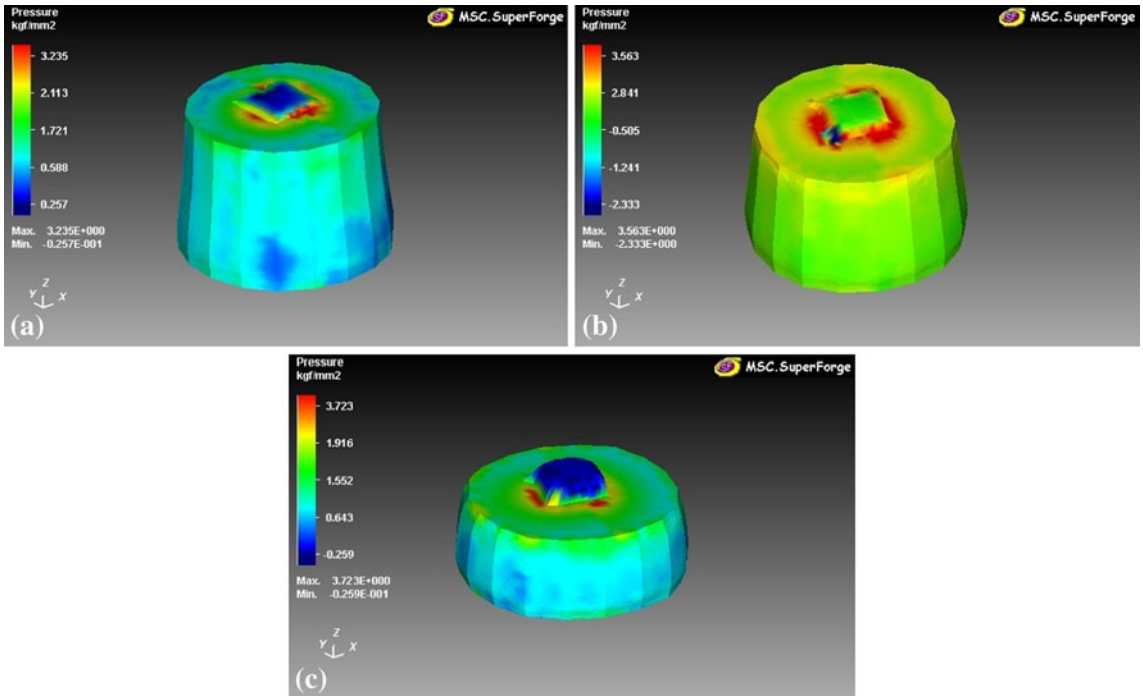

Fig. 6 FEM contour (stress distribution) on square die-orifice for (a) 10% deformation, (b) 30% deformation, and (c) 50% deformation

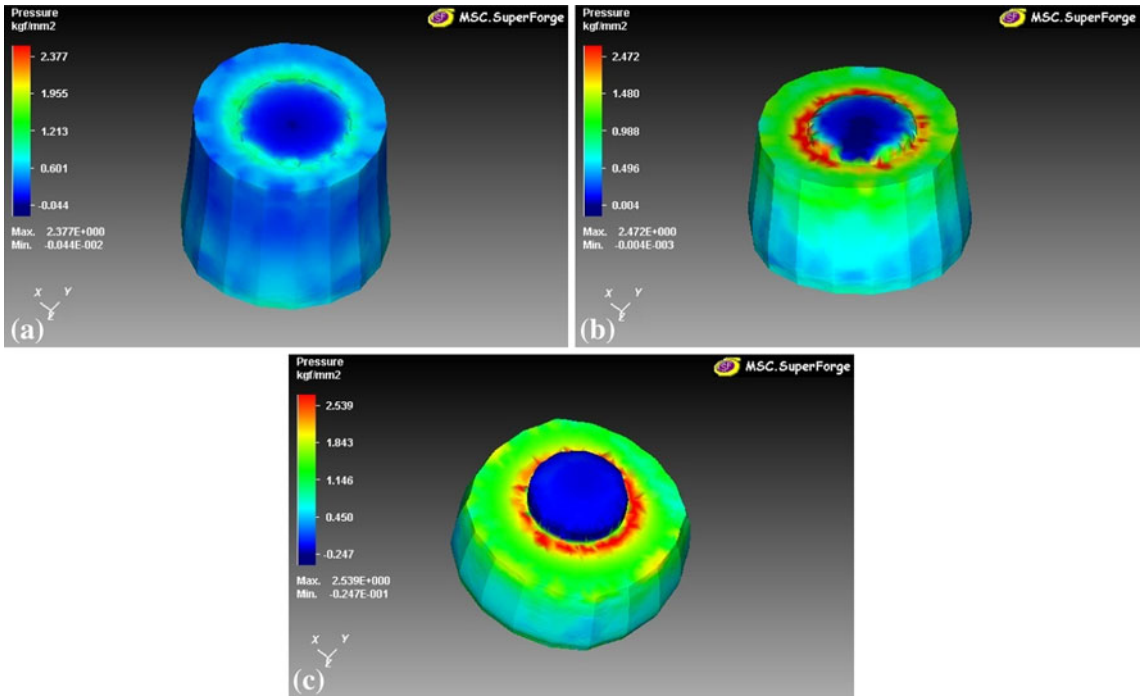

Fig. 7 FEM contour (stress distribution) on circular die-orifice for (a) 10% deformation, (b) 30% deformation, and (c) 50% deformation

As the dies moves upwards and downwards to shape and extrude the workpiece, bulging occurs due to the friction occurring between the dies and workpiece material. By forcing the punch down onto the material to change its original shape, frictional forces cause stresses in the *X*, *Y*, and *Z* directions and high tension forces occur along the *Z* direction. As seen from the plotted results, the pressures are higher along the entire edges of the square orifice in considering the overall shaping process. The material flows more freely through the orifice due to low frictional resistance, and it is similar to the states of kinetic and static friction near the upper and bottom die, respectively, as reported elsewhere (Ref 7).

5.2 Circular Die Orifice

Figure 7(a-c) shows the pressure distributions for 10, 30, and 50%, respectively, during the extrusion-forging process for the circular die orifice. The maximum stress occurred at 2,377

for 10% deformation and it reached to 2,472 and 2,579 N/mm^2 for 30 and 50% deformations, respectively. From the results it can be observed that the effect of pressures on the edges of cylindrical orifice seem to be less significant than the pressures in the square orifice. For example, as the maximum pressure occurred along the edges of square orifice was 3.235 (Fig. 6a) for 10% deformation, however, it was 2.377 (Fig. 7a) at circular orifice for the same reduction, and pressure values increased with increasing stroke or deformation (%). The similar results are also reported in Ref 19. From the comparison of Fig. 6(b) and 7(b), as the maximum pressure is 2.863 N/mm^2 for square and 2,463 N/mm^2 for circular orifices, and this value goes up to 3,723 for 50% deformation at square and to 2,539 at circular orifices. That means, the higher extrusion loads required for square orifice than circular die orifice during the metal flow. In other word, low pressure enables the metal to flow easier moving through the orifice hence enabling the extrusion process easier, however, this can be lowered further by radiuses at orifice edges. The pressure accumulation on the edges of the circular orifice is less effective than that on the square orifice up to 50% deformation.

5.3 The Extrusion-Forging Forces

Figure 8 shows the variation of maximum extrusion-forging loads in comparison with UBM and FEM and experiments for square and circular orifice at constant friction, $m = 0.23$. The results of experiments having reduction values up to 50% deformation for the square and circular orifices were plotted in comparison with theoretical predictions. It is seen that the first degree of deformation occurred, and the required forces increased with increasing deformation (%). The value of $m = 0.23$ was determined experimentally by ring test and was used in theoretical analyses. Figure 9 shows the influence of deformation and friction on extrusion force in comparison with UBM and FEM for circular and square orifices. The required extrusion forging force for square orifice was higher than forces required for circular and extrusion force predictions were found to be slightly higher in UBM than FEM predictions.

It is seen that extrusion load increases with increasing deformation and friction. As also shown in Ref 7, although not studied here, it was reported that the bulging increases with increasing pressures in the extruded part (Ref 17). The required forming forces increased due to increased pressures along inner die walls (Ref 18). The total deformation for the billet which was extruded through the square orifice appeared to be slightly higher than for the circular orifice. Although the values of cross-sectional areas of the orifices used in experiments are identical, due to the corners of square orifice, the forming loads appeared to be slightly larger than that of the circular orifice. It should be noted that the shape complexity of the square orifice, which is the ratio between the perimeter and its closure length, is greater than that of circular orifice. Therefore, the metal flow in the axial direction is restricted and material tends to flow in the radial direction. Although the UBM curves appear to be a bit higher than the FEM and experimental results, the trends are fairly in good agreement. This is because the UBM is based on the upper bounds of the geometry.

From the analysis it can be seen that the trends of extrusion-forging force predictions are in good agreement with experimental results (Fig. 8) for the square and cylindrical dies. The pressure force acting along the edges of square dies is more effective at higher deformation; however, in the circular die orifice, it appears to be more effective along the whole surface of square section for all reductions, and this means greater shaping force is required. From the comparison from the FEM and UBM analyses it was seen that both the methods have some advantageous and disadvantages over each other, for example, the UBM provides extremely rapid load predictions, while FEM provides adequate modelling and pressure distributions. The results of FEM analysis are closer to the experiments than the UBM results (Fig. 9). As expected, and also reported in Ref 13, the required extrusion forces are higher in UBM than the experiments and FEM analysis, due to ignorance of some process parameters such as temperature, forces of inertia, and so on. Although small deviations between the both theories and experiments are observed, the both theoretical predictions employing the proposed models (UBM and FEM) are qualitatively agreed with the experiments.

5.4 Influence of Friction

Effect of friction factor on extrusion-forging force was also investigated theoretically and compared with experiments. Figure 10 shows the influence of friction on extrusion force for the square and circular die orifices. Total punch force increases with increasing deformation rate (%) and friction factor due to the frictional portion of the total pressure in the UBM and FEM solutions. Since no lubricant used during experiments, the friction factor was determined as $m = 0.23$ using the ring test and this value was used in theoretical studies. From the figures, it can be said that by increasing friction factor for both circular and square orifices, the role of friction becomes more significant. For example for 10% deformation,

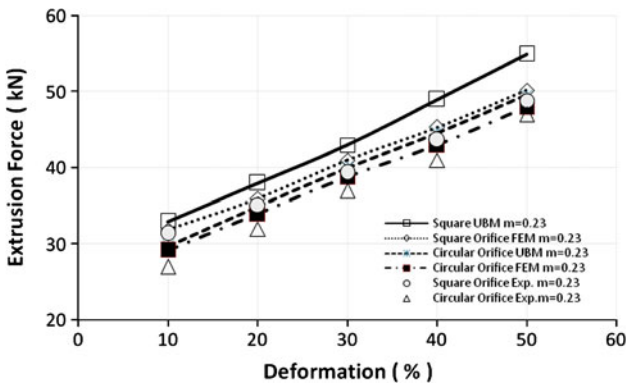

Fig. 8 The variation of extrusion force with deformation (%) for square and circular die-orifices

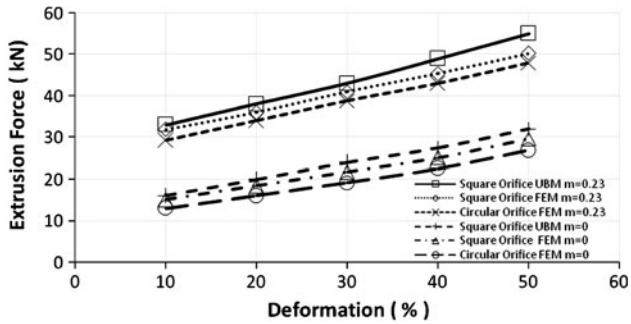

Fig. 9 Comparison of extrusion-forging forces with deformation (%) for square and die-circular orifices

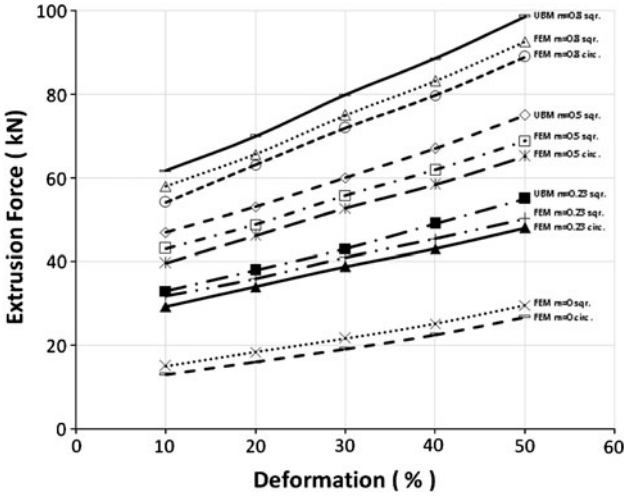

Fig. 10 Effect of friction and deformation on forming forces

as the required (predicted) extrusion force is 31.5 and 29.2 kN for $m = 0.23$ in square and circular orifices, it increased to 57 and 54 kN for $m = 0.8$, respectively. As shown in Fig. 10, the friction has great influence on required extrusion forces, however, as also shown here, although some difference in forming requirement, it was shown that the die shape has no great effect in required extrusion force (Ref 7). The overall results of this study may be used in design of complex die profiles in extrusion-forging processes.

6. Conclusions

It can be concluded from this study that the UBM and FEM methods have some advantages and disadvantages over each other. As the UBM appears to be a much faster solution for predicting the required forming force when compared to FEM; however, FEM is a more adequate method for physical modelling and evaluating the pressure distribution of a deforming body. Both FEM and UBM exhibited fairly good agreement with experiments. It was shown that the required load in forging-extrusion is influenced by the orifice geometry and extrusion load in circular orifice was found to be lower than square orifice. The current analyses can be used to predict the required forming load and material flow to produce square and cylindrical cross sections during extrusion-forging processes and so will help the designer to improve die and various product designs. Such analyses are also promising in automation of forging-extrusion process and can be extended to design more complex extrusion products.

References

1. G.W. Rowe, *Principals of Industrial Metalworking Processes*, Edward Arnold Publishers Ltd, London, 1977
2. H. Kudo, Some Analytical Experimental Studies of Axisymmetric Cold Forging and Extrusion, *Int. J. Mech. Sci.*, 1960, **2**, p 71–117
3. L. Brayden and J. Monaghan, An Analysis of Closed Die Extrusion Forging, *J. Mater. Process. Technol.*, 1991, **26**, p 141–157
4. M.S.J. Hashmi and F.B. Klemz, Axisymmetric Extrusion Forging: Effects of Material Property and Product Geometry, *Int. J. Mach. Tool Des. Res.*, 1986, **26**, p 157–170
5. J. Vickery and J. Monaghan, An Analysis of Closed Die Extrusion Forging, *J. Mater. Process. Technol.*, 1994, **55**, p 103–110
6. S.C. Jain, A.N. Bramley, C.H. Lee, and S. Kobayashi, Theory and Experiments in Extrusion Forging, *Proc. 11th MTDR Conf. Birmingham*, 1970, p 1097–1115
7. G. Maccarini, C. Giardini, G. Pellegrini, and A. Bugini, The influence of Die Geometry on Cold Extrusion Forging Operations: FEM and Experimental Results, *J. Mater. Process. Technol.*, 1991, **27**, p 227–238
8. C. Giardini, E. Ceretti, and G. Maccarini, Formability in Extrusion Forging: The Influence of Die Geometry and Friction Conditions, *Mater. Process. Technol.*, 1995, **5**, p 302–308
9. Y.W. Chun and C.H. Yuan, The Influence of Die Shape on the Flow Deformation of Extrusion Forging, *J. Mater. Process. Technol.*, 2002, **124**, p 67–76
10. W. Hu and M.S.J. Hashmi, Study of Metal Flow in Extrusion Forging of Rectangular Billet, *J. Mater. Process. Technol.*, 1994, **43**, p 51–59
11. B. Aksakal, S. Sezek, and Y. Can, Forging of Polygonal Discs Using the Dual Stream Functions, *Mater. Des.*, 2005, **26**(8), p 643–654
12. S. Sezek, B. Aksakal, and Y. Can, Analysis of Cold and Hot Plate Rolling Using Dual Stream Functions, *Mater. Des.*, 2008, **29**, p 584–596
13. T. Altinbalik and O. Ayeri, A Theoretical and Experimental Study for Forward Extrusion of Clover Sections, *Mater. Des.*, 2008, **29**(6), p 1182–1189
14. B.C. Hwang, H.I. Lee, and W. Bae, A UBET Analysis of the Non-Axisymmetric Combined Extrusion Process, *J. Mater. Process. Technol.*, 2003, **139**, p 547–552
15. M.B. Jooybari, M. Saboori, M.N. Azad, and S.J. Hosseinipour, Combined Upper Bound and Slab Method, Finite Element and Experimental Study of Optimal Die Profile in Extrusion, *Mater. Des.*, 2007, **8**, p 1812–1818
16. C. Combeaud, Y. Demay, and B. Vergnes, Experimental Study of the Volume Defects in Polystyrene Extrusion, *J. Non-Newtonian Fluid Mech.*, 2004, **121**, p 175–185
17. L. Hua and X. Han, 3D FE Modelling of Cold Rotary Forging of a Ring Workpiece, *J. Mater. Process. Technol.*, 2009, **209**, p 5353–5362
18. M. Arentoft, N. Bay, P.T. Tang, J.D. Jensen, A New Lubricant Carrier for Metal Forming, *CIRP Ann. Manuf. Technol.*, 2009. doi:10.1016/j.CIRP
19. H.I. Lee, B.C. Hwang, and W.B. Bae, A UBET Analysis of Non-Axisymmetric Forward and Backward Extrusion, *J. Mater. Process. Technol.*, 2001, **113**, p 103–108